Spatio-temporal dynamics of the basin scale internal waves in Lake Simcoe

Damien Bouffard, Leon Boegman

Environmental Fluid Dynamics Laboratory,
Department of Civil Engineering, Ellis Hall, 58 University Ave. Kingston, ON
K7L 3N6 Canada
damien.bouffard@queensu.ca

Abstract

Lake Simcoe (Canada) suffers from eutrophication and hypoxia, resulting from excessive phosphorus loads. A better understanding of the physical processes responsible for mixing and transport in the lake is needed to analyse the spatial and temporal variability of the phosphorus concentrations. Field data and three-dimensional numerical simulations were used to determine the dynamics of the basin scale internal waves in this medium sized lake. The hydrostatic Reynolds-averaged Navier-Stokes equation model, ELCOM, was found to correctly simulate the seasonal stratification and the internal wave field. The dominant response to the wind forcing is a counter clockwise Kelvin wave (period, T ~ 3.5 days) and a clockwise Poincaré wave (T ~ 14 h). Both Kelvin and Poincaré wave periods and energy contents match published analytical descriptions for a flat bottomed elliptical lake.

1. Introduction

Lakes, as enclosed natural systems, provide an ideal framework for the study of physical processes in stratified fluids. In lakes, wind energy excites basin scale internal waves (Bouffard and Boegman, 2011) whose spatial and temporal dynamics drive flux paths of biogeochemical substances (Imberger 1998).

Lake Simcoe (Canada, Fig. 1) suffers from eutrophication and hypoxia, resulting from excessive phosphorus loads. While the distribution of phosphorus loads has been intensively studied in Lake Simcoe (Winter et al., 2007), the dynamics of basin-scale mixing processes, in distributing these loads within the lake remain unknown. The objective of this study is to provide a first description of the Lake Simcoe hydrodynamics. We focus in this paper on the basin scale internal waves as they are a key feature in transport and mixing in stratified lakes.

We thank Jörg Imberger at the Center for Water Research from providing the ELCOM code and David Evans (Trent University) for providing 2008 field data. This project was funded by the Environment Canada Lake Simcoe Clean-Up Fund.

2. Methods

We apply the three-dimensional Estuary and Lake Computer Model (ELCOM) to Lake Simcoe during the ice free season of 2008. ELCOM solves the unsteady hydrostatic Reynolds-averaged Navier-Stokes equations 500 m x 500 m horizontal z-level grid with vertical grid spacing between 0.5 m and 1 m. A one-dimensional mixed-layer model is used for turbulence closure of vertical Reynolds stress terms (Hodges et al. 2000). The model is forced with 1-hour meteorological data (wind speed and direction, relative humidity, air temperature) recorded over the lake surface (Environment Canada station 45151 , Fig. 1) , and

long and short wave radiation and precipitations recorded at Egbert Care (< 20 km from Lake Simcoe). The most important inflows are also incorporated in the model.

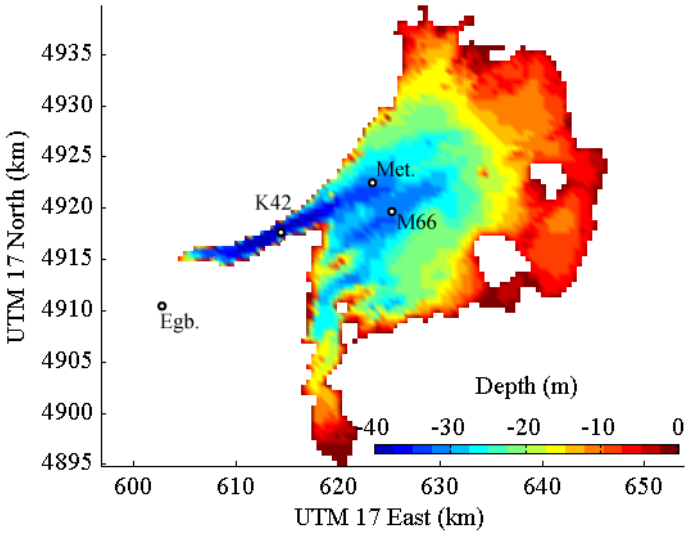

Figure 1: Map of Lake Simcoe. Field stations (K42 and M66) and meteorological stations (Met. and Egb) are shown.

The model was compared to observed temperature timeseries data recorded during the ice free season at various depths at two stations with a 15 min sampling period. The model was also compared to temperature profiles collected every month at 8 stations throughout the lake (not shown, data from Ontario Ministry of the Environment). Model skill was determined with both graphical comparisons and statistical quantities, including the root-mean-square-error (RMSE),

$$RMSE = \left(\frac{1}{M} \sum_{j=1}^{M} \frac{1}{N} \sum_{i=1}^{N} (m_{ij} - o_{ij})^{0.5} \right)^2 \quad (1)$$

where m and o represent the model and field temperature data respectively and M and N are the number of thermistors and N the time steps of the investigated mooring (K42 or M66).

Kinetic energy, KE and available potential energy, APE, of the basin scale internal waves are inferred from the band pass filtered velocity current and isotherm displacement data

$$KE = \int_S \int_z 0.5\rho\left(u^2 + v^2\right) dz dS \quad (2)$$

$$APE = \int_S \rho g' \eta^2 dS \quad (3)$$

with ρ, u, v, g' and η being respectively the water density, the eastern and northern current velocity, the reduced gravity and the isotherm displacement.

3. Results

3.1 Model validation

With an RMSE (Eq. 1) of 0.8 and 1.1°C for stations K42 and M66, ELCOM correctly simulates the seasonal stratification over Lake Simcoe. Contours of the modelled temperature profiles are compared to the observed temperatures in Fig. 2 and confirms the ability of the model to reproduce the spatial and temporal variability observed in Lake Simcoe. While internal waves with short amplitude and period are observed in the offshore station located in the main basin (M66), the nearshore station located in the western bay (K42) has a drastically different dynamics with large internal waves travelling in the thermocline. Such difference is

also noticeable in the power spectra with station K42 having a large peak around 90 h and station M66 having a large peak around 14 h. Each peak is present both in the model and the observed data (Fig. 3).

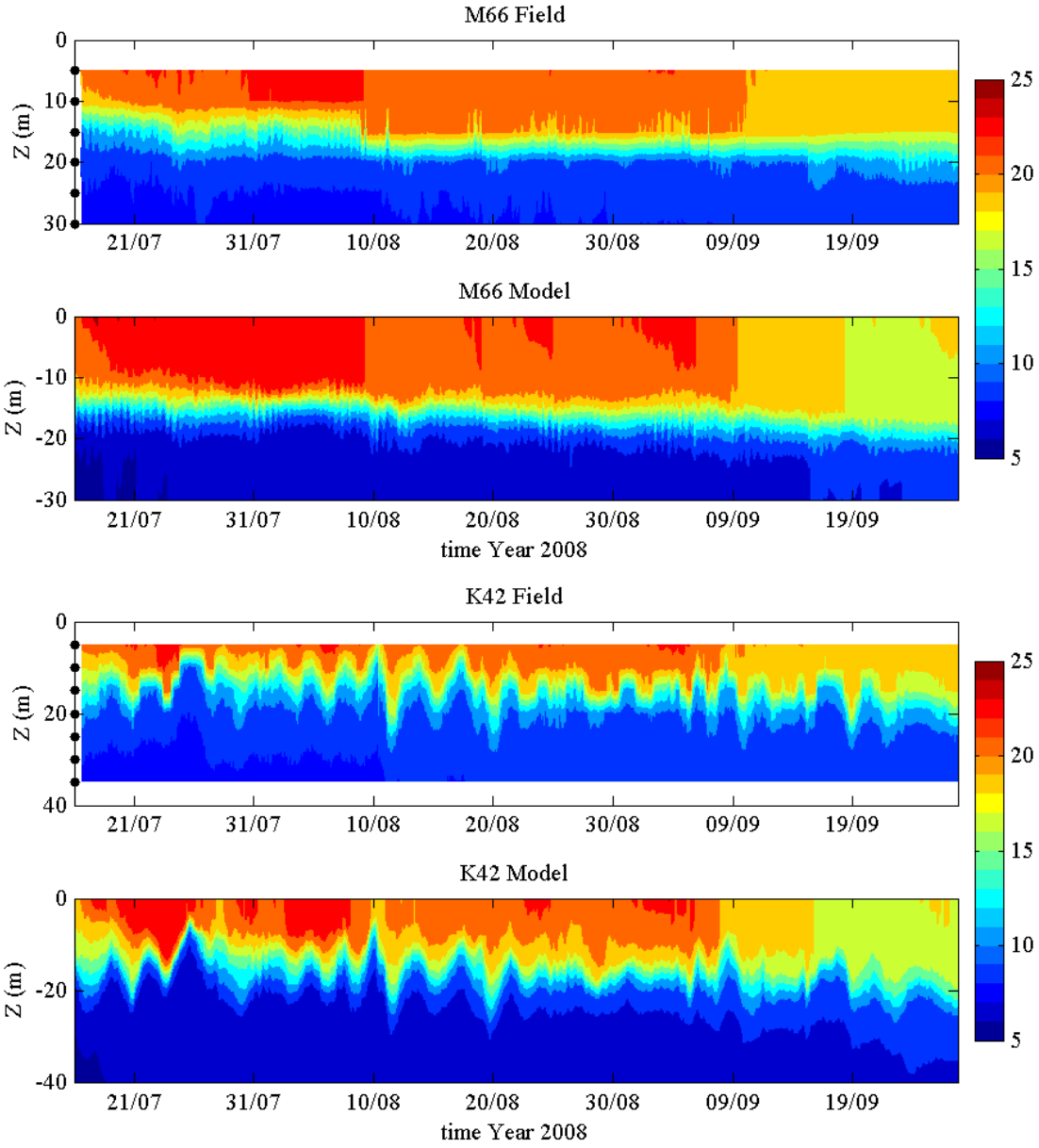

Figure 2: Observed (a and c) and modelled temperature contours at stations M66 (a and b) and K42 (c and d) .Depths of the thermistors are indicated with black bullets in a and c. Vertical axis (*Z*) is depth and the colorbar is temperature in degrees Celsius.

3.2 Basin Scale Internal waves

The influence of the Earth's rotation on the internal wave field is quantified according to the Burger number $S = c/fL$, where c is the phase speed of the non rotating internal wave (Merian equation), L a length scale of the basin, usually taken as half of the width and f the inertial frequency. For lake Simcoe, we found $S \sim 0.26 < 1$ and the Earth's rotation will affect the dynamics of the internal waves.

The low frequency peak (period, T ~ 90 h) is identified as a Kelvin wave propagating counter-clockwise along the shore (Fig. 4a). The amphidromic point and isophase lines (Fig. 4a) indicate the travel of the Kelvin wave. The secondary peak at T ~ 14 h is identified as a Poincare wave propagating clockwise (Fig. 4b) and has its maximum of current velocity in the offshore part of the lake.

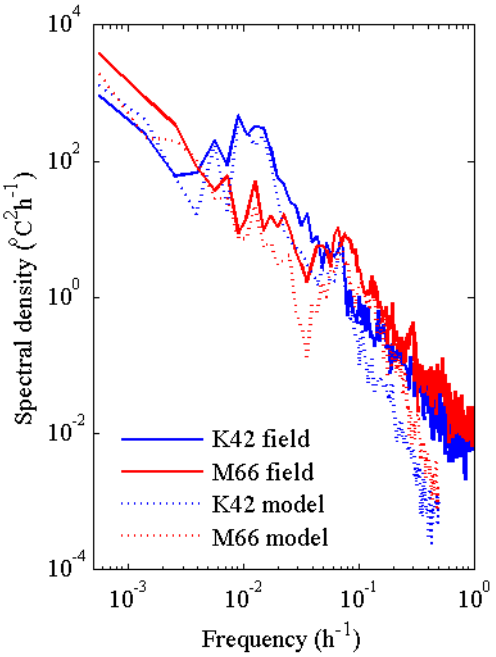

Figure 3: Spectral energy of modelled and observed temperature at stations K42 and M66.

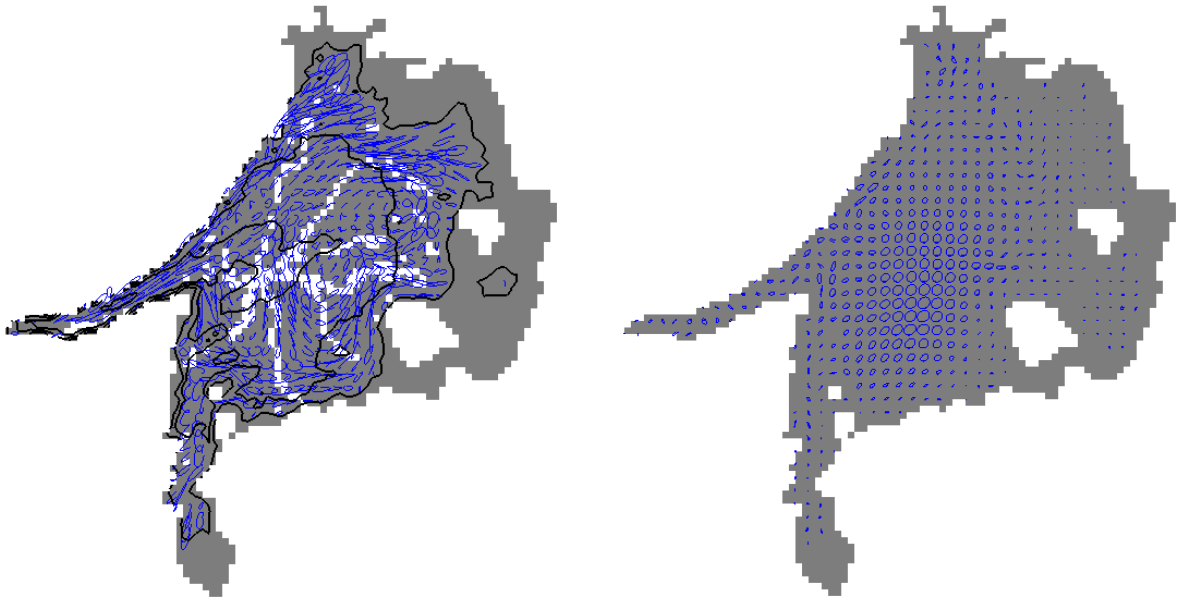

Figure 4: Progressive vector plot of velocity current (at depth, Z =12 m) over a) one Kelvin wave period (~ 90 h) and b) over one Poincare wave period (~14 h). Velocity currents have been band pass filtered around the wave period of interest. Black lines in a) indicates the bathymetry (10 m spacing) and white lines indicate different lines of constant phase (isophases). The time interval between two isophases is T/5. The Kelvin wave exhibits a strong counter clockwise alongshore current and the Poincare wave shows current movement in clockwise near-inertial circles.

KE and APE have been estimated at each model cell and integrated over the whole basin. In the present study, we focus on a 16 day period (5/2008 to 21/2008) that includes a strong western wind event with an average wind speed of 6.2 ms^{-1} between 6 and 10 August. Another short strong western wind event is recorded two days later on 12 August. Such winds energize the basin scale internal wave field; as can be seen in Fig. 2.

Results shown in Fig. 5 indicate that 70% of the total basin scale internal wave energy is contained in the Kelvin wave. The ratio between APE and KE for each basin scale internal wave indicates that Poincare waves and Kelvin wave store the energy differently. Over the16 day period investigated, the average ratio APE/KE is about 1.3 for the Kelvin wave and 0.3 for the Poincare wave. Contrary to internal waves not affected by rotation (e.g. internal seiches or linear high frequency internal waves), there is no equipartition of energy between KE and APE in the case of rotational linear internal waves.

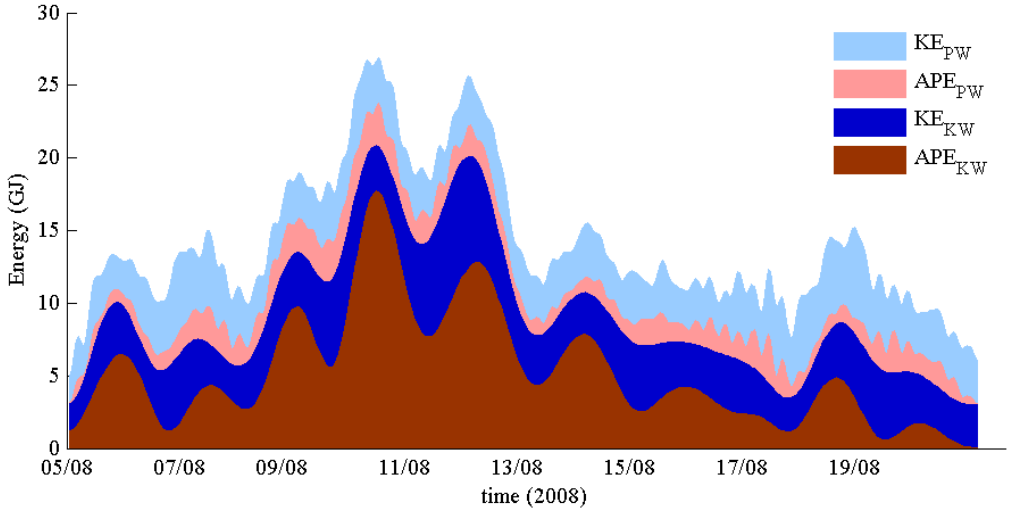

Figure 5: Time evolution of the energy stored in the basin scale internal waves during the 16 day period. The accumulated rate of work done by wind during this period is 288 GJ.

4. Discussion and conclusion

Our results are compared to the analytical solution for an elliptical basin described in Antenucci and Imberger (2001). They show that the wave period associated with the basin scale internal wave can be expressed as a function of the Burger number and the basin shape at the thermocline depth. Note that the Burger number account for the stratification (through c) and will vary during the ice free period in Lake Simcoe. As the Poincare wave was found to travel only in the main basin (Fig 4b) we fit an elliptical of ratio 2:3 to the main basin and apply the analytical model, which predicts a Poincare wave period of $T_{PW}=Ti/(1+0.09S+4.67S^2-0.346S^3)$ = 13.7 h, very close to the observed period for this wave.\

As the Kelvin wave was found to travel in the western bay (Fig 4a), any elliptical basin fit becomes difficult and we simply apply the Merian formula, $T_{KW} = 2L/c$ where L is the length of the basin including the western bay. This estimate leads to T_{KW} ~ 89 h during the highly stratified period - again close to the observed period of 90 h.

The Antenucci and Imberger (2001) analytical model also predicts the partitioning of energy between the potential and the kinetic forms. Using their analytical model, we estimate PE/KE

~ 0.2 for the Poincare wave and 1.2 for the Kelvin wave. These values are very close to the 0.3 and 1.3 from our results, confirming therefore, the applicability of using the flatted bottom elliptical model for lakes with irregular bathymetry and shape.

Our ratio between the total energy stored in the Kelvin wave and the Poincare wave is compared to the analytical work from Stocker and Imberger (2003) using a circular flat basin. They found that in the case, S ~ 0.26, the ratio is about 4, which is higher than the ratio of 1.4 we found, but both results indicate that the Poincare wave component is less important than the Kelvin wave.

In conclusion, we found that ELCOM successfully simulates the dynamics of Kelvin and Poincare waves in Lake Simcoe. To entirely close the energy budget and compare it to the energy input by the wind, the geostrophic component of the circulation has to be taken into account; as does the flux to high-frequency internal waves, which are below the grid scale. For a lake with Burger number near 0.3, Stocker and Imberger (2003) estimated that 30% of the energy is stored in the geostrophic component and 70% in the basin scale internal wave field. Similarly, for non rotational lakes, Boegman et al (2005) found that as much as 20% of the wind input can be found in high-frequency internal waves. The distribution for waves in rotational systems remains unknown.

References

Antenucci, J. and Imberger, J. (2001). Energetics of long internal gravity waves in large lakes *Limnol. Oceanogr.*, 46**,** 1760-1773.

Boegman, L., Ivey, G.N. and Imberger, J. (2005). The energetics of internal wave degeneration in lakes. *J. Fluid. Mech.* 531: 159-180.

Bouffard, D. and Boegman, L. (2011). Basin scale internal wave. Encyclopedia of Lakes and Reservoirs. Springer.(Accepted).

Hodges, B. R., J. Imberger, A. Saggio and K. B. Winters. (2000). Modeling basin-scale internal waves in a stratified lake. *Limnol. Oceanogr.*, 45**,** 1603-1620.

Imberger, J. (1998) Flux paths in a stratified lake: a review. In Physical Processes in Lakes and Oceans (ed. J. Imberger), Coastal and Estaurine Studies, vol. 54, pp. 1–18. AGU

Stocker, R. and Imberger, J. (2003). Energy partitioning and horizontal dispersion in a stratified rotating lake, *J. Phys. Oceanogr.*, 33, 512-529

Winter, J. G., M. C. Eimers, P. J. Dillon, L. D. Scott, W. A. Scheider and C. C. Willox. (2007). Phosphorus inputs to lake Simcoe from 1990 to 2003: declines in tributary loads and observations on lake water quality. *J. Great lakes Res.*, 33, 381-396